# UNEP IMEO Technical Documentation for Methane Satellite Detection and Quantification

## 1. Introduction

UNEP's International Methane Emissions Observatory (IMEO) launched the Methane Alert and Response System (MARS) in a pilot phase at COP-27 and a fully-operational phase at COP-28. MARS increases transparency and accelerates implementation of the Global Methane Pledge (GMP) by bringing together four critical components: (1) satellite detection of large sources of anthropogenic methane emissions, (2) notification of relevant stakeholders about these detected emissions, (3) assessment and mitigation of emission events and (4) tracking and documentation of events, including public sharing of data.

Building a comprehensive understanding of where methane emissions come from and how those emissions change over time is widely considered critical to realize deep reductions in methane emissions. UNEP IMEO is leveraging the state of the art of current remote sensing technologies to detect and localize very large point source emissions from human activity (energy, waste, agriculture). The rapid expansion of satellite capability is increasingly allowing for the detection of lower emissions rates at increased frequency and detection of area source emissions (e.g., from agriculture).

This document provides an overview of the scientific principles and methodologies employed by UNEP IMEO and its partner organizations to *detect* and *quantify* methane point source emissions from satellites. While this document is not comprehensive in its descriptions, additional information can be found in the published scientific literature citations found throughout this document. UNEP IMEO satellite methane data is published via the UNEP IMEO Methane Data portal.

## 2. Basic Scientific Principles

The general principles of methane detection from satellites can be found in Jacob *et al.,* (2016; 2022). Below we summarize the main points from these principles.

Methane detection from space relies on the basic principles of imaging spectroscopy. Atmospheric methane is detectable because it absorbs radiation in the shortwave infrared (SWIR) at 1.65 and 2.3 μm, and in the thermal infrared (TIR) at 8 μm. **Figure 1**shows the atmospheric optical depths (AOD) of trace gasses in the atmosphere. Both SWIR channels are used for satellite remote sensing because the methane signal can be unambiguously determined as other atmospheric trace gasses do not obscure the absorption spectra. As shown in Figure 1, while the absorption strength for methane at 2.3 μm is stronger than at 1.65 μm, solar radiation is 3 times weaker at the former wavelength. Because TIR measurements are mostly sensitive to methane in the upper atmosphere, these types of measurements are less useful for understanding methane emissions that occur at the Earth's surface.

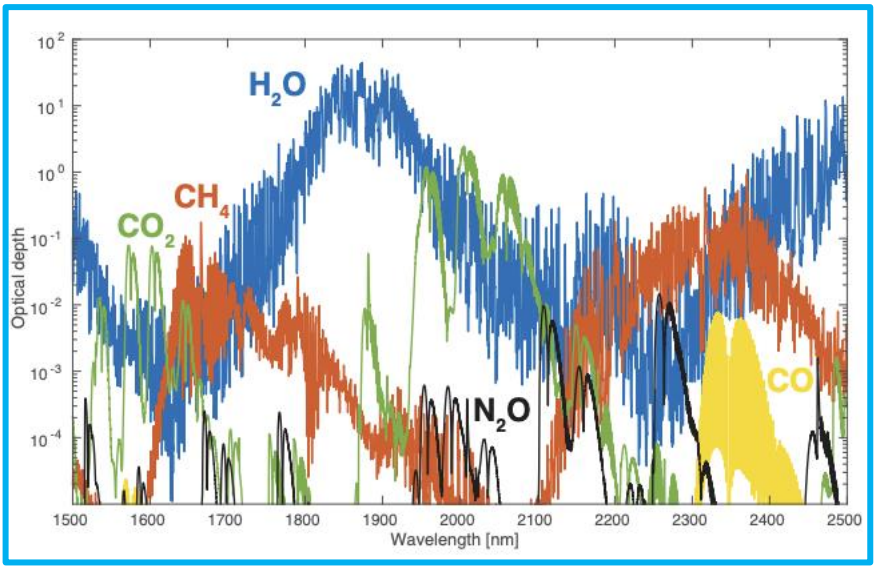


**Figure 1:** Atmospheric optical depth (AOD) of major trace gasses for the US Standard atmosphere showing methane detection channels in the SWIR (Figure 4 from Jacob et al., 2016)

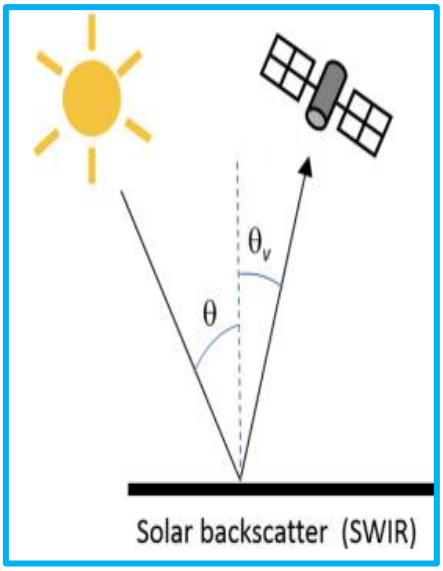


**Figure 2:** Configuration of passive SWIR satellites ($\theta$ and $\theta_v$ are solar zenith and satellite viewing angles; from Jacob et al., 2019 Figure 2)

Most methane-detecting satellites are *passive* – they rely on reflected sunlight from the surface and atmosphere to provide a signal (**Figure 2**). To retrieve methane at either SWIR channel, the reflected solar spectrum measured by the satellite is fit to a modeled spectrum, normalized by the geometric air mass factor, and the total vertical column density of methane is determined ($\Omega$; molecules $cm^{-2}$). Note that the measured slant column density is normalized by the geometric air mass factor ($cos^{-1}\theta + cos^{-1}\theta_v$; where $\theta$ and $\theta_v$ are the solar and satellite viewing angels, respectively) to account for the viewing geometry of the satellite. Finally, to remove the sensitivity of $\Omega$ to surface pressure changes, $\Omega$ is converted to a dry air column-average mole fraction or column-average mixing ratio ($X_{CH4} = \Omega/\Omega_a$ where $\Omega_a$ is the vertical column density of dry air from the local pressure and humidity).

Because methane-detecting satellites rely on reflected sunlight for their signal, they have some innate detection limitations. First, the presence of clouds inhibits the detection of sunlight reflection from the surface, making near-surface methane undetectable over cloudy pixels. Nighttime observations are not possible, and high-latitude observations are difficult during low-sunlight conditions due to the lack of reflected solar signal. Dark surfaces, such as over water or in densely forested regions, absorb incoming solar radiation and reduce the amount of radiation reflected to the satellite, making detection more difficult, but not impossible depending on specific sensor characteristics and sun angle. Heterogenous surfaces, such as in mountainous regions or in cities, can also increase the difficulty for methane retrieval.

## 3. Methane-Detecting Satellite Characteristics

Most methane-detecting satellites are generally **Low Earth Orbit** (LEO; altitude of 2000 km or less) and **sun-synchronous** (cover each area of the world at a constant local time of day) to maximize the signal of reflected sunlight. These types of satellites revolve around the Earth, imaging along a **swath** (area imaged on surface). They also have **revisit periods** – the time it takes for the satellite to return and reimage the same location on the Earth – which is a function of both the satellite orbit and its ability to target or not (see below). There is now the capability to also use some **geostationary** weather satellites (Watine-Guiu et al., 2023) to detect very, very large methane emissions; these types of satellites are at such a high altitude that they orbit the Earth at its rotation speed, thus continuously imaging a portion of the Earth's surface (e.g., over the Americas). More general

information on satellites and remote sensing is available from the Canada Center for Mapping and Earth Observation, Natural Resources Canada.

Methane can be emitted from either ***area sources*** or ***point sources***. Area sources can be both *diffuse* (e.g., emissions from wetlands over the area of the wetland) or can represent the integral of a very large number of individually small emitters (e.g., cumulative emissions from low-production oil wells; *Omara et al.*, 2022). Point sources represent emissions, for example, from a single facility or piece of equipment within a facility, (e.g., a single facility emitting > 100 kg methane per hour; *Duren et al.*, 2019).

Following *Jacob et al.*, (2022), methane-detecting satellites can be classified in terms of their ability to observe methane on global- and regional-scales, as well as by their capability to determine emissions from area sources or on the scale of individual point sources. **Figure 4**, adapted from Jacob *et al.*, (2022), describes these classifications pictorially.

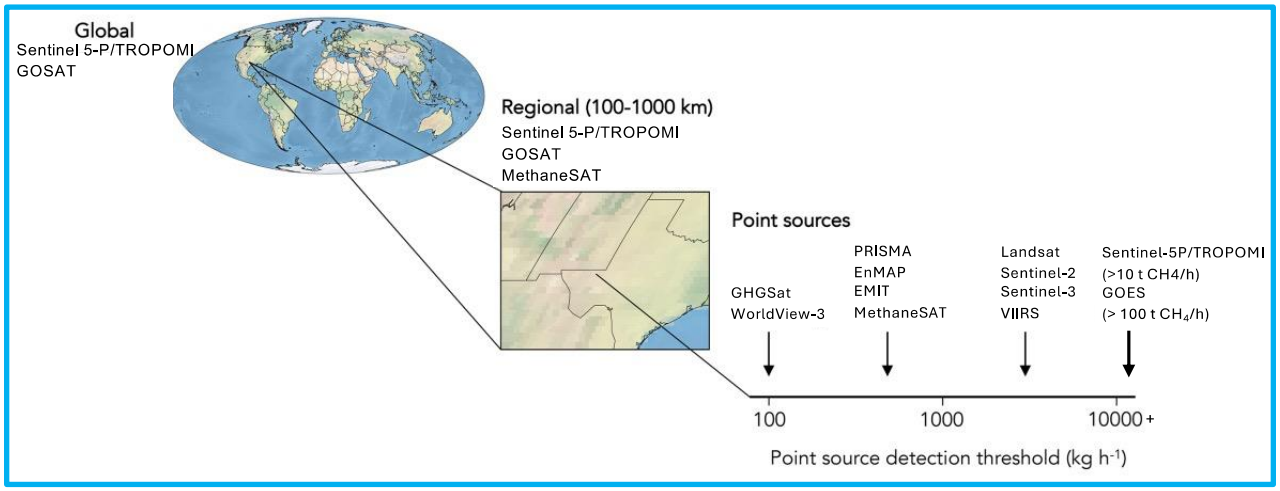


**Figure 4:** Satellite classification for global mapping, area flux (regional) and point source imaging satellites. Point source detection thresholds (i.e., Minimum Detection Limits (MDL) in ideal observing conditions) are shown by order of magnitude. Figure adapted from *Jacob et al.*, 2022 their Figure 4).

**Global mapping satellites** – such as the European Space Agency's (ESA) Sentinel-5P/TROPOMI satellite – typically have lower spatial-resolution pixels but very frequent return times, frequent global coverage, and a high sensitivity for detecting methane. These types of satellites can be used for global-to-regional emissions using **inverse flux inversion methods** (*Jacob et al.*, 2022). Averaging time series of $X_{CH4}$ retrievals from these type of instruments, including utilizing wind-rotation techniques, is useful for locating **'hot-spots'**, or regions of enhanced methane concentration resulting from one or more persistent emissions sources (Maasakkers *et al.*, 2022). Additionally, these satellites can detect very large (> 10 tonnes methane per hour) point source emissions (*Lauvaux et al.*, 2022). UNEP IMEO uses these types of instruments for both use cases – determining **Regions of Interest** (ROI) to explore with high-resolution point source imagers and for finding very large point source emission plumes.

**Point source imagers** typically have very high spatial resolution with pixels of 60 m or less. Because of this characteristic, methane emissions plumes obtained from these instruments are attributable at the facility-scale. These types of instruments can either take data *continuously* or be *tasked* (*targeted*). Because of their resolution and narrow swath width, *continuously* viewing point source imagers can only view the same location on the Earth after several days. *Targeted* or *tasked* satellites view limited locations provided by end users.

Between **point source imagers** and **global mapping satellites** are **area flux mappers**, such as MethaneSAT from the Environmental Defense Fund (EDF) and New Zealand Space Agency's. These instruments have higher spatial

resolution than global mappers, but similarly high sensitivity to methane. However, they typically take data over limited regions of the Earth, such as only over major oil and gas producing basins. These instruments can determine emissions from both *area* and *point sources.*

UNEP IMEO uses this existing suite of Earth Observation satellites (**Figure 5**) to detect, localize, and quantify large human emission sources globally. Data from these satellites is publicly available, though in many cases specialized remote sensing expertise is required to properly interpret these data. UNEP provides this expertise to the global community to help further the goals of the Global Methane Pledge. Figure 5 and **Table 1**, adapted from *Jacob et al.,* (2022), provide information on the satellites with publicly available data useful for detecting methane.

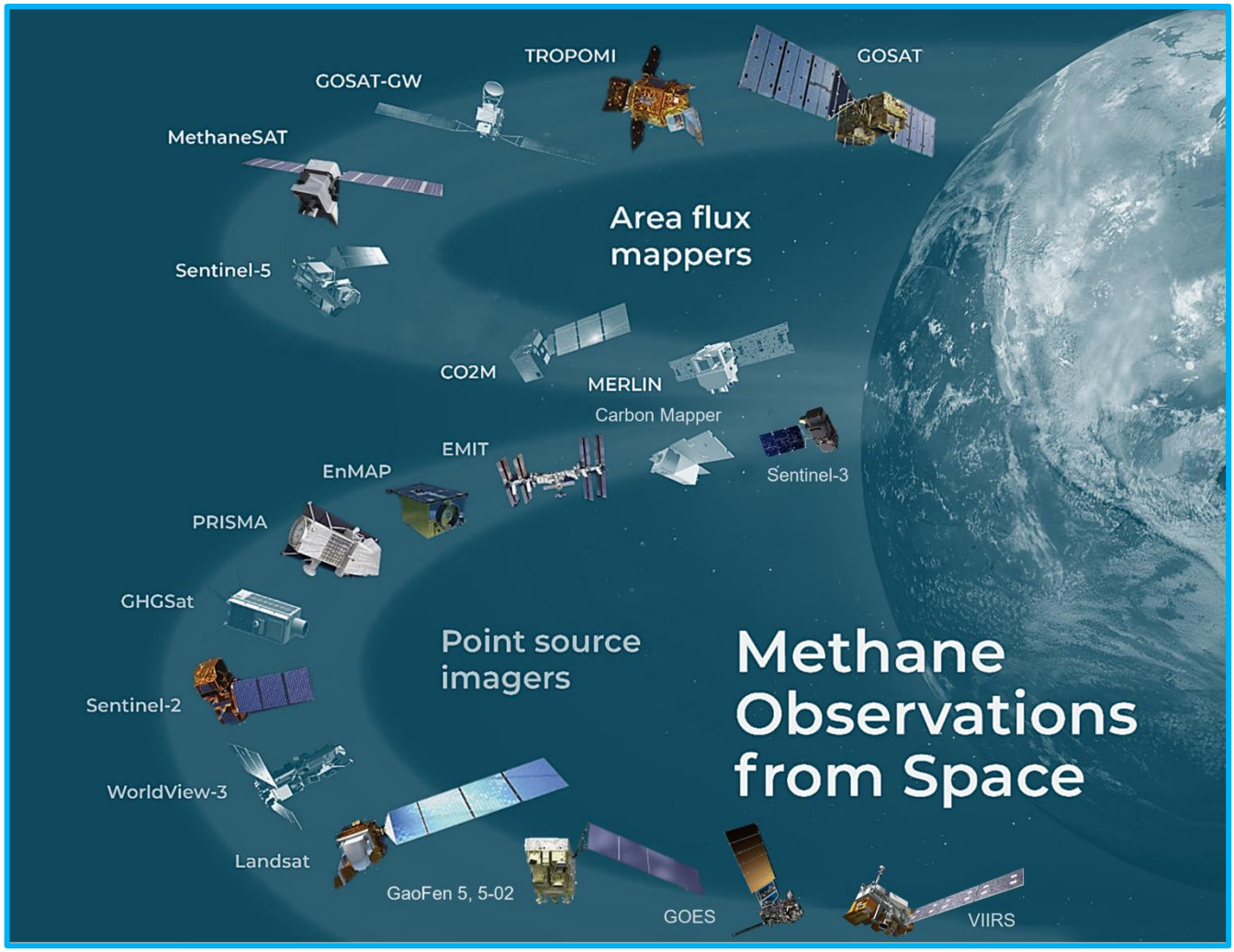


**Figure 5:** Methane-sensing satellites used by UNEP IMEO (shown in color; non-colored satellites represent future public satellite missions useful for UNEP IMEO and commercial satellites with non-public data (GHGSat, WorldView-3). Information on future satellites and commercial satellites is available through the CEOS GHG Satellite Missions Portal. Figure adapted from *Jacob et al.,* 2022.

Additional information on methane-sensing satellites, including from the private sector and not-yet launched, can be found on the Greenhouse Gas Satellite Missions portal from the Committee on Earth Observation Satellites (CEOS).

## 4. Retrieval Methodologies

Here we describe, briefly, methodologies for retrieving $X_{CH4}$ (column-average methane mixing ratio) from the satellites used by UNEP IMEO. These methodologies vary depending on the instrument type. While UNEP IMEO provides these retrievals for most of the satellites in Table 1, others are provided by partner organizations (SRON and Kayrros).

**TROPOMI Hot-Spots.** The European Space Agency (ESA) provides an operational $X_{CH4}$ data product using a full-physics retrieval detailed in *Hasekamp et al., (2022)*. To this product, the Netherlands Institute for Space Research (SRON) has developed regularization and posteriori correction schemes based on TROPOMI $X_{CH4}$ data to reduce biases in the data due to, for example, surface albedo (*Lorente et al.*, 2021). This corrected data product forms the basis for the determination of **'hot-spots'** – locations with persistently enhanced methane concentrations based on long-term averages of TROPOMI $X_{CH4}$ data (*Maasakkers et al., 2022*). A wind-rotation technique, in which for a target point, data is rotated on individual days based on the wind direction at 10 m such that the wind vector always aligns north, allows localization of methane sources when the downwind concentration is consistently enhanced compared to the upwind concentration. UNEP IMEO uses TROPOMI hot-spots to direct *targeting* and *monitoring* (*Vaughan et al., 2023*) of locations of high-probability methane emissions with high-spatial resolution satellites.

**Table 1:** Current Methane-Detecting Satellites used by UNEP IMEO

| Type[a] | Agency[b] | Satellite System | Launch Year | Pixel Resolution [km] | Approximate Minimum Detection Limit (MDL)[c] [tonnes $CH_4$ per hour] | Approximate Return Time [days][d] | Tasking[e] |
|---|---|---|---|---|---|---|---|
| **Global Mapper** | ESA | Sentinel-5P/TROPOMI[f] | 2017 | 7 × 5.5 | 10 | 1 | N |
| | JAXA, MOE, NIES | GOSAT[g] | 2009 | 10 (diameter; circular pixels) | 10 | 3 | N |
| **Geostationary** | NOAA | GOES[h] | 2016 | ~2 × 2 | 100 | 5-10 minutes | N |
| **Area Mapper** | EDF | MethaneSAT | 2024 | 0.20 × 0.40 | 2-3 | 3-4 | Y |
| **Point-Source Imager** | ESA | Sentinel-2 | 2015 | 0.02 × 0.02 | 1 | 2-5 | N |
| | ESA | Sentinel-3 | | 0.50 × 0.50 | 10 | 1 | N |
| | NOAA, NASA | VIIRS | 2011 | 0.75 × 0.75 | 10 | < 1 | N |
| | NASA, USGS | Landsat-8/9 | 2013 | 0.03 × 0.03 | 1 | 16 | N |
| | ASI | PRISMA | 2019 | 0.03 × 0.03 | 0.5 | 4 | Y |
| | DLR | EnMAP | 2022 | 0.03 × 0.03 | 0.5 | 4 | Y |
| | CNSA | GaoFen-5 | 2018 | 0.03 × 0.03 | 0.5 | 5 | Y |
| | NASA | EMIT[i] | 2022 | 0.06 × 0.06 | 0.3 | 3 | N |

[a]Classification as **Global Mapper** (near-daily global coverage, lower-spatial resolution, high precision), **Area Mapper** (medium-spatial resolution, high-precision instrument for area emissions and point source emissions), **Point Source Imagers** (high-resolution with pixel size on order of 60 m or less; useful for localization of emissions to facility scale; can be *targeted* or *continuously monitoring*), and **Geostationary** (very high-frequency, low-spatial resolution observations over a region of globe; can quantify total event emissions and not just instantaneous emission rate).

[b]JAXA = Japan Aerospace Exploration Agency, MOE = Ministry of Environment, NIES = National Institute for Environmental Studies, ESA = European Space Agency, NASA = National Aeronautics and Space Administration, DLR = Deutsches Zentrum für Luft-und Raumfahrt, USGS = United States Geological Survey, ASI = Agenzia Spaziale Italiana, NOAA = National Oceanic and Atmospheric Administration, CNSA = China National Space Administration

[c]**Minimum Detection Limit (MDL)** is level below which satellite is unable to detect emissions; note that inability to observe does not necessarily indicate that emissions don't exist, as they may be below the MDL. MDLs are a function of sensor characteristics *and* environmental/observing conditions. Generally, they are provided for the best observing conditions (homogenous, bright, dry surface with no vegetation, no clouds, and moderate wind). Further from these ideal conditions, the detection limit will be higher.

[d]Time interval between successive viewings of the same scene/location on Earth's surface.

[e]Targeted or tasked instruments take data over provided locations, rather than continuously everywhere along orbit.

[f]Sentinel-5P is used by UNEP IMEO both to provide methane **'hot-spots'** (regions of elevated methane concentration) for high-resolution satellite targeting, and for providing large (> 10 tonnes $CH_4$ per hour) methane plume (point source) emissions data.

[g]GOSAT data is low-resolution and used to provide 'hot-spot' data for high-resolution satellite targeting.

[h]GOES is a **geostationary** satellite providing near-continuous observations over the Americas; it is used to monitor very, very large (> 100 tonnes $CH_4$ per hour) emissions events and to target high-resolution satellites. Resolution is 1 km × 1 km to 2 km × 2 km. Because it takes data nearly-continuously, event integrated emissions can be determined.

[i]EMIT is an instrument aboard the International Space Station (ISS). It has coverage between +51.6°N and 51.6°S.

**TROPOMI Methane Point Sources.** Kayrros SAS uses bias-corrected Level 2 TROPOMI $X_{CH4}$ data from ESA, to which they apply an automatic background estimation and plume detection algorithm described by *Lauvaux et al., (2022).* TROPOMI plumes have a localization error of approximately ±50 km, so these plumes themselves are not attributable to facility-scale unless plumes are either in regions with sparse potential emissions sources or are coincidentally viewed with other high-resolution satellites, particularly those with nearly contemporaneous overpass times (e.g., Sentinel 3 *Pandey et al., 2023*; VIIRS *de Jong, et al., 2024*).

**High-resolution hyperspectral satellites**. Satellites such as PRISMA, EnMAP, EMIT or GaoFen-5 combine high spatial resolution (30 m × 30 m to 60 m × 60 m) and high spectral resolution. They feature numerous spectral channels keyed to methane's strong methane absorption features around 2300 nm. Methane retrievals from these satellites are computed using a **Match-Filter (MF)** approach, as detailed in numerous scientific papers (PRISMA *Guanter et al., 2021*; EnMAP Roger et al., 2023, 2024; ; GaoFen-5 *Irakulis-Loitxate et. al., 2021*), involves detecting methane's absorption spectrum using statistics extracted from the hyperspectral image. Radiative transfer simulations are subsequently utilized to derive per pixel methane concentrations. Most of these missions require a tasking process, *i.e.,* data users must specify in advance the locations of interest and make targeted requests. UNEP IMEO applies the MF retrieval method to derive methane from L1B satellite radiance data provided by the respective space agencies.

**High-resolution multispectral satellites.** Satellites such as Sentinel-2, Landsat-8, Sentinel-3 or GOES, offer frequent and extensive observations across vast regions, albeit with a lower sensitivity to methane due to their lower spectral resolution. Under certain favorable observation conditions, such as strong emissions and background homogeneity, methane retrievals can be performed using the **Multi-Band-Multi-Pass (MBMP)** approach. This method, as detailed in studies by *Varon et. al.* (2021), *Irakulis-Loitxate et al.*, (2022a,b); *Pandey et. al.* (2023), *Gorroño et al.*, (2023) and *Watine-Guiu et. al.* (2023), leverages the varying levels of absorption in various shortwave infrared spectrum bands when methane is in the satellite's line of sight. Radiative transfer simulations are similarly employed to derive per pixel methane concentrations ($X_{CH4}$). UNEP IMEO applies the MBMP retrieval method to derive methane from L1B or L1C satellite radiance data provided by the respective space agencies.

## 5. Plume Masking and Emissions Estimation

Quantification of methane emissions from a single satellite observation center on estimating the instantaneous source rate (*Q*; mass methane emitted per time unit), reflecting the emission rate at the time of observation. Emissions from a point source produce a turbulent 'plume' whose shape and extent depend on the emissions source strength, the wind, and atmospheric turbulence (a function of atmospheric stability and surface roughness; *Varon et al., 2018*). **Figure 6** from *Shuit et al., (2023)* shows some examples of methane plumes from lower- and higher-spatial resolution methane-detecting satellites (i.e., global mapping versus point source imager).

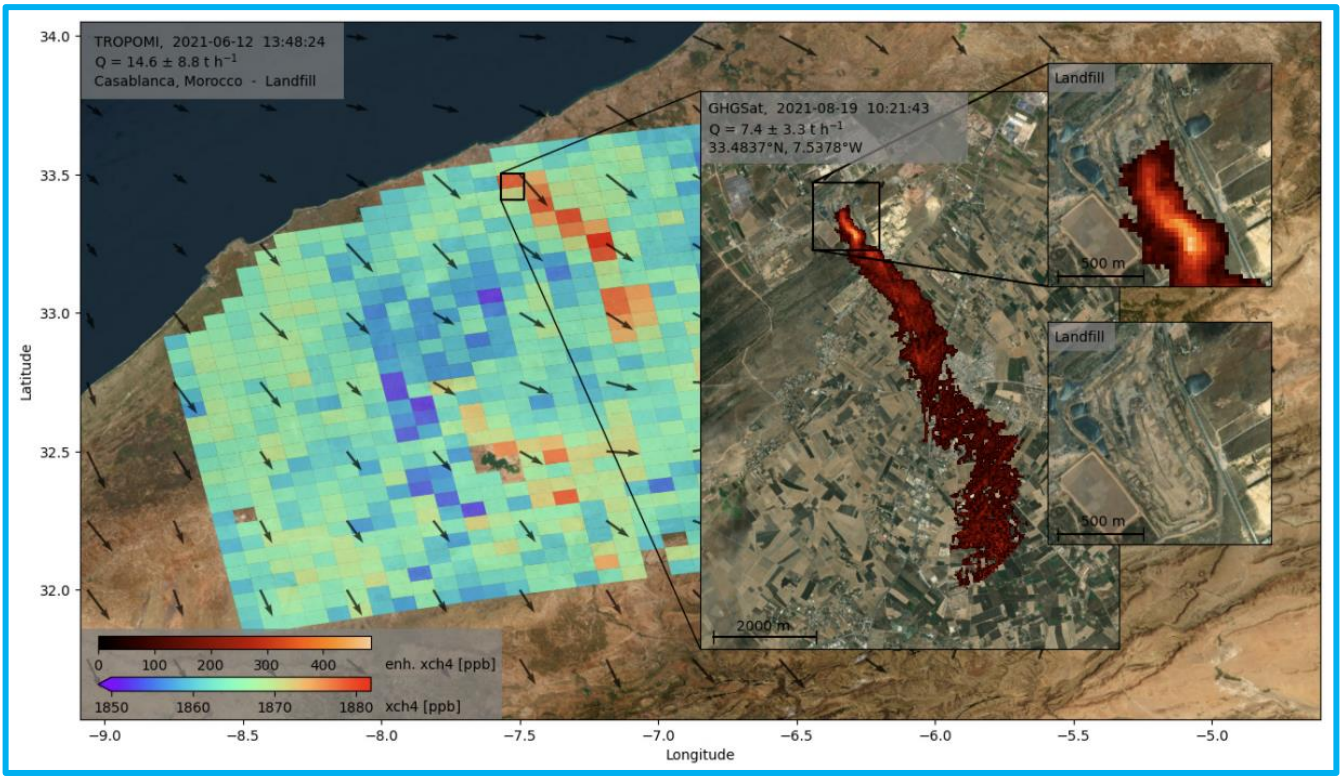


**Figure 6:** Methane plumes from Sentine-5P/TROPOMI (lower-spatial resolution global mapping satellite) and GHGSat (commercial high-spatial resolution point source imager. Figure from *Schuit et al., (2023*; their Figure 8).

Before estimating plume emissions, for many quantification methodologies a **plume 'mask'** must be determined. The plume mask represents the physical extent of the plume, and it is determined through pixel selection procedures that separate signal from noise. Statistical algorithms, machine learning algorithms, and human evaluation can be used to construct such masks that consider only the pixels with significant signal-to-noise ratios within a scene to be part of a methane plume.

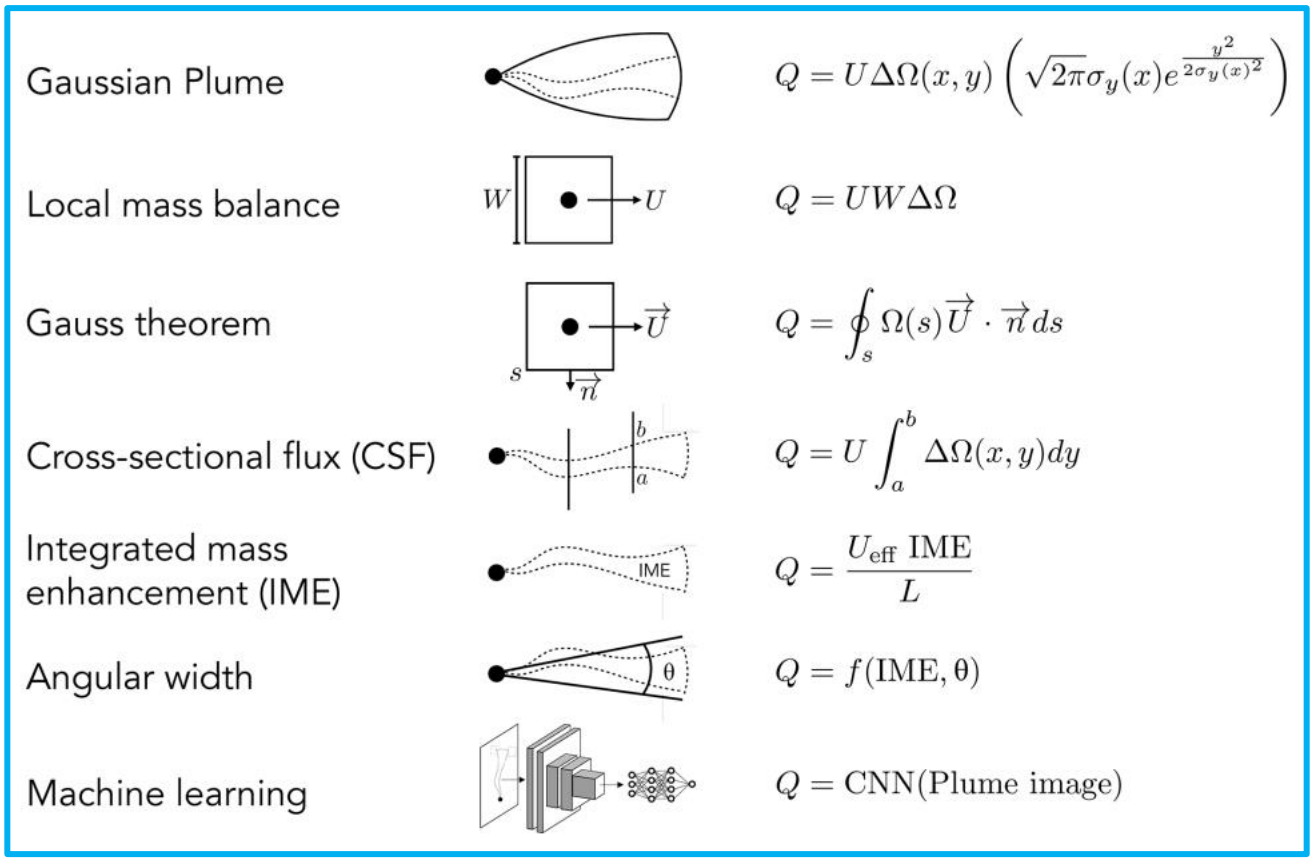


**Figure 7:** Pictorial representation of methods used to quantify point source emission rates (Q; mass per unit time) from point source imagers. UNEP IMEO uses the IME method described below. Figure from *Jacob et al., (2022*; their Figure 6) with additional details on other methodologies available in that reference.

Multiple-methodologies can be used to infer point-source emission rates (*Q*) from satellite data. **Figure 7** from *Jacob et al., (2022)* illustrates these methods and more details on each can be found in that reference. UNEP IMEO utilizes the **Integrated Mass Enhancement (IME)** method, which calculates the total mass of methane by integrating the concentration detected in each pixel over the entire area of the observed plume. To determine the source rate, an empirical linear relationship is applied, incorporating the effective wind speed and the length of the plume, as described by *Frankenberg et. al.* (2016):

$$Q = \frac{U_{eff}IME}{L}$$

where *Q* is the point source emission rate [kg $s^{-1}$], $U_{eff}$ [m $s^{-1}$] is the effective wind speed – itself a function of the 10 m wind speed and surface turbulence characteristics, and *L* [m] is the horizontal extent of the plume. Additional details on the IME algorithm are found in *Varon et al., (2018).*

## 6. Emissions Uncertainties and Validation

**Plume misidentification errors: False positives** occur when a methane plume is determined to exist when no plume exists. This can occur, for example, when reflection from a surface feature appears as a plume-like structure in the satellite reflectance data. **False negatives** occur when a plume exists but is not detected. Such detection errors are more likely when plume detection and masking is performed solely using computer algorithms (statistical or AI-enhanced). False negatives can also occur when the emission flux rate is at the edge of the detection limit of the satellites, and there is insufficient confidence to determine if the observed

enhancement is an emission without additional information. At UNEP IMEO, while some deep-learning models are used to initially detect plumes (Vaughan *et al.,* 2023), a trained expert analyst *always* provides quality control on *every* plume published to avoid these types of errors.

**Quantification errors:** Sources of error for point source emission quantification include the extent of the plume (*L*), which depends on the plume mask determination, and, more importantly, the effective wind speed $U_{eff}$. Low wind speeds make emissions estimation difficult because, though they improve signal-to-noise, the plume length (*L*) determination is difficult. Very high wind speeds are difficult because quicker dispersion potentially makes the plume more difficult to be observed. Because measured wind data is generally not available locally, the 10-m wind speed ($U_{10}$) from reanalysis data is generally used. These operational data, provided by meteorological and space institutions such as the European Center for Midrange Weather Forecasting or the NASA Global Modeling and Assimilation Office, introduce representational error because they are only available at lower resolution (e.g., 10- or 25-km grids). This representation error ranges between 15 to 50% depending on satellite sensor precision and environmental conditions (wind speed) at the time of observation (*Varon et al.* 2018). At UNEP IMEO, we capture the representation error introduced by reanalysis winds by computing *Q* using winds from multiple reanalysis models. This uncertainty is reflected in the uncertainty estimate for every emission rate provided.

**Validation:** Point source quantification methodologies, as applied to the date from satellites in use by UNEP IMEO, have been validated by single-blind controlled release studies (*Sherwin et al., 2023a*, *b*). In these studies, methane is released with a metered rate at a known location and time. Multiple teams of experts applied various quantification methodologies to satellites including Sentinel-2, Landsat, PRISMA, EnMAP, and GaoFen-5 to estimate emissions from these sites without knowing the actual metered rate, if methane was released or not, and with and then without knowledge of local wind speeds. Overall, satellites were found to perform similarly to aircraft in terms of quantification error (i.e., within ±50% of the metered value). Minimum detection limits are 1 to 3 orders of magnitude higher than aircraft due to the significantly greater distance of satellites to the emission source. However, the controlled released studies thus far have taken place in regions with high-quality observing conditions (desert region with low cloud cover, high surface albedo, low surface heterogeneity, remote from other potential emission sources, and favorable wind conditions). In those conditions, satellite performance is expected to be at its highest, with commensurately low Minimum Detection Limits (MDL). Future studies, sponsored by UNEP IMEO, will extend these controlled release studies to account for variable observing conditions to better test satellite performance in less-than-ideal cases, and to test a wider range of metered release rates. To compensate for the lack of controlled release experiments in other scenarios and in different observing conditions, satellite measurements are also validated and recalibrated using simulations with synthetic plumes (*Gorroño et al.,* 2023).

## 7. References

Duren, R.M., Thorpe, A.K., Foster, K.T., Rafiq, T., Hopkins, F. M., Yadav, V., Bue, B. D., Thompson, D. R., Conley, S., Colombi, N. K., Frankenberg, C., McCubbin, I., B., Eastwood, M. L., Falk, M., Herner, J. D., Croes, B. E., Green, R. O., and C. E. Miller (2019), California's methane super-emitters. *Nature*, 575, 180–184, doi:10.1038/s41586-019-1720-3.

Gorroño, J., Varon, D. J., Irakulis-Loitxate, I., and Guanter, L., (2023), Understanding the potential of Sentinel-2 for monitoring methane point emissions, *Atmos. Meas. Tech.*, 16, 89–107, doi.org/10.5194/amt-16-89-2023.

Guanter, L., Irakulis-Loitxate, I., Gorroño, J., Sánchez-García, E., Cusworth, D. H., Varon, D. J., Cogliati, S., and R. Colombo, (2021), Mapping methane point emissions with the PRISMA spaceborne imaging spectrometer, *Remote Sensing of Environment*, 265, 112671, doi.org/10.1016/j.rse.2021.112671.

Hasenkamp, O., Lorente, A., Hu, H., Butz, A., de Brugh, J. A., and J. Landgraf, (2022), Algorithm Theoretical Baseline Document for Sentinel-5 Precursor Methane Retrieval, SRON document number SRON-S5P-LEV2-RP-001.

Irakulis-Loitxate, I., Guanter, L., Maasakkers, J., Zavala-Araiza, D., and I. Aben, (2022a), Satellites detect abatable super-emissions in one of the world's largest methane hotspot regions, *Environ. Sci. Technol.,* 56, 4, 2143-2152, doi:10.1021/acs.est.1c04873.

Irakulis-Loitxate, I., Gorroño, J., Zavala-Araiza, D., and L. Guanter (2022b), Satellites detect a methane ultra-emission event from an offshore platform in the Gulf of Mexico, *Environ. Sci. Technol. Lett.,* 9, 6, 520-524, doi:10.1021/acs.estlett.2c00225.

Jacob, D. J., Varon, D. J., Cusworth, D. H., Dennison, P. E., Frankenberg, C., Gautam, R., Guanter, L., Kelley, J., McKeever, J., Ott, L. E., Poulter, B., Qu, Z., Thorpe, A. K., Worden, J. R., and Duren, R. M., (2022), Quantifying methane emissions from the global scale down to point sources using satellite observations of atmospheric methane, *Atmos. Chem. Phys*., 22, 9617–9646, doi.org/10.5194/acp-22-9617-2022.

Jacob, D. J., Turner, A. J., Maasakkers, J. D., Sheng, J., Sun, K., Liu, X., Chance, K., Aben, I., McKeever, J., and Frankenberg, C., (2016), Satellite observations of atmospheric methane and their value for quantifying methane emissions, *Atmos. Chem. Phys.*, 16, 14371–14396, doi.org/10.5194/acp-16-14371-2016.

de Jong, T. A., Maasakkers, J. D., Irakulis-Loitxate, I., Randles, C. A., Tol, P., and I. Aben, (2024), Daily global methane super-emitter detection and source identification with sub-daily tracking [preprint], *Earth ArXiv*, doi:10.31223/X51M52.

Lauvaux, T., Giron, C., Mazzolini, M., D'Aspremont, A., Duren, R., Cusworth, D. H., Shindell, D., and P. Cias, (2022), *Science*, 375, 6580, 557-561, doi:10.1126/science.abj4351.

Lorente, A., Borsdorff, T., Butz, A., Hasekamp, O., aan de Brugh, J., Schneider, A., Wu, L., Hase, F., Kivi, R., Wunch, D., Pollard, D. F., Shiomi, K., Deutscher, N. M., Velazco, V. A., Roehl, C. M., Wennberg, P. O., Warneke, T., and Landgraf, J., (2021), Methane retrieved from TROPOMI: improvement of the data product and validation of the first 2 years of measurements, *Atmos. Meas. Tech*., 14, 665–684, doi.org/10.5194/amt-14-665-2021.

Maasakkers, J. D., Varon, D. J., Elfasdóttir, A., McKeever, J., Jervis, D., Mahapatra, G., Pandey, S., Lorente, A., Borsdorff, T., Foorthuis, L., R., Schuit, B. J., Tol, P., van Kempen, T., A., van Hees, R., and I. Aben, (2022), Using satellites to uncover large methane emissions from landfills, *Science Advances*, 8, 32, doi:10.1126/sciadv.abn9683.

Omara, M., Zavala-Araiza, D., Lyon, D.R., Hmiel, B., Roberts, K. A., and S. P. Hamburg, (2022), Methane emissions from US low production oil and natural gas well sites, *Nat Commun,* 13, 2085, doi.org/10.1038/s41467-022-29709-3.

Pandey, S., van Nistelrooij, M., Maasakkers, Pratik Sutar, J. D., Houweling, S., Varon, D. J., Tol, P., Gains, D., Worden, J., and I. Aben, (2023), Daily detection and quantification of methane leaks using Sentinel-3: a tiered satellite observation approach with Sentinel-2 and Sentinel-5P, *Remote Sensing of Environment*, 296, 113716, doi.org/10.1016/j.rse.2023.113716

Roger, J., Guanter, L., Gorroño, J., and Irakulis-Loitxate, I., (2024a), Exploiting the entire near-infrared spectral range to improve the detection of methane plumes with high-resolution imaging spectrometers, *Atmos. Meas. Tech*., 17, 1333–1346, doi.org/10.5194/amt-17-1333-2024.

Roger, J., Irakulis-Loitxate, I., Valverde, A., Gorroño, J., Chabrillat, S., Brell., M., and L. Guanter, (2024b), High-Resolution Methane Mapping With the EnMAP Satellite Imaging Spectroscopy Mission, *IEEE Transactions on Geoscience and Remote Sensing*, 62, 1-12, doi:10.1109/TGRS.2024.3352403.

Schuit, B. J., Maasakkers, J. D., Bijl, P., Mahapatra, G., van den Berg, A.-W., Pandey, S., Lorente, A., Borsdorff, T., Houweling, S., Varon, D. J., McKeever, J., Jervis, D., Girard, M., Irakulis-Loitxate, I., Gorroño, J., Guanter, L., Cusworth, D. H., and Aben, I., (2023), Automated detection and monitoring of methane super-emitters using satellite data, *Atmos. Chem. Phys.*, 23, 9071–9098, doi.org/10.5194/acp-23-9071-2023.

Sherwin, E.D., Rutherford, J.S., Chen, Y., Aminfard, S., Kort, E. A., Jackson, R. B., and A. R. Brandt (2023a), Single-blind validation of space-based point-source detection and quantification of onshore methane emissions, *Sci Rep,* 13, 3836, doi:10.1038/s41598-023-30761-2.

Sherwin, E. D., El Abbadi, S. H., Burdeau, P. M., Zhang, Z., Chen, Z., Rutherford, J. S., Chen, Y., and Brandt, A. R. (2024), Single-blind test of nine methane-sensing satellite systems from three continents, *Atmos. Meas. Tech*., 17, 765–782, doi.org/10.5194/amt-17-765-2024.

Varon, D. J., Jervis, D., McKeever, J., Spence, I., Gains, D., and Jacob, D. J., (2021), High-frequency monitoring of anomalous methane point sources with multispectral Sentinel-2 satellite observations, *Atmos. Meas. Tech*., 14, 2771–2785, doi.org/10.5194/amt-14-2771-2021.

Varon, D. J., Jacob, D. J., McKeever, J., Jervis, D., Durak, B. O., Xia, Y., and Huang Y., (2018), Quantifying methane point sources from fine-scale satellite observations of atmospheric methane plumes, *Atmos. Meas. Tech*., 11, 5673-5686, doi:10.5194/amt-11-5673-2018.

Vaughan, A., Mateo-García, G., Gómez-Chova, L., Růžička, V., Guanter, L., and Irakulis-Loitxate, I., (2023), CH4Net: a deep learning model for monitoring methane super-emitters with Sentinel-2 imagery, *EGUsphere* [preprint], doi.org/10.5194/egusphere-2023-563.

Watine-Guiu, M., Varon, D.J., Irakulis-Loitxate, I., Balasus, N., and D. J. Jacob (2023), Geostationary satellite observations of extreme and transient methane emissions from oil and gas infrastructure, *Proceedings of the National Academy of Sciences*, 120, 52, doi:10.1073/pnas.2310797120.